Available online at www.sciencedirect.com
SCIENCE DIRECT®
Thin Solid Films 441 (2003) 223–227
thin solid films
www.elsevier.com/locate/tsf

4-(Dicyanomethylene)-2-*t*-butyl-6-(1,1,7,7-tetramethyljulolidyl-9-enyl)-4*H*-pyran doped red emitters in organic light-emitting devices

Tswen-Hsin Liu, Chung-Yeh Iou, Shih-Wen Wen, Chin H. Chen*

Microelectronics and Information Systems Research Center and Department of Applied Chemistry, National Chiao Tung University Hsinchu, Box 1055, Hsinchu, Taiwan 300, R.O.C.

Received 17 September 2002; received in revised form 19 March 2003; accepted 16 May 2003

Abstract

We have studied the device optimization of red 4-(Dicyanomethylene)-2-*t*-butyl-6-(1,1,7,7-tetramethyljulolidyl-9-enyl)-4*H*-pyran (DCJTB) dye doped Alq_3 emitters in organic light-emitting devices (OLED). By varying the hole injection materials, thickness of hole-transport layer and by evaporation with rubrene as co-dopant, efficiencies of 3.24 cd/A and near saturated CIE color coordinates of $x=0.643$, $y=0.354$ was achieved without needing additional doping of hole-trap with NPB. From experiments with film thickness variation, it is concluded that the improved electrofluorescent (EL) performance and color saturation are due to the synergistic effects of microcavity, device structural optimization as well as optimal doping of DCJTB with rubrene. We believe this luminance efficiency for red is by far one of the best ever reported for dye-doped electrofluorescent OLEDs.
© 2003 Elsevier B.V. All rights reserved.

Keywords: Organic light emitting devices; Electroluminescence

1. Introduction

Organic light-emitting devices (OLED) have received considerable attention due to their potential application in flat-panel displays. For full color display applications, it is necessary to demonstrate a set of primary red, green, blue emitters with sufficiently high luminous efficiencies of proper proportion and a matching set of chromaticity in order to achieve a desired white emission with the right CIE coordinates. Such emitters can, in principle, be obtained using a guest-host doped system utilizing a single host matrix dispersed with various RGB guest dopants leading to EL of desirable hues [1]. Typically, the green OLED emitter has the highest efficiency [2] followed by the blue [3], which leaves red as the weakest link in the triad whose balanced overall luminance can be critical in the making of a good full color passive matrix [4] as well as active matrix display [5].

An archetypical red dopant material used for many of today's OLED displays on the market is 4-(dicyanomethylene)-2-*t*-butyl-6-(1,1,7,7-tetramethyljulolidyl-9-enyl)-4*H*-pyran, better known as DCJTB [6]. Despite the fact that DCJTB is an excellent red fluorescent dye with solution PL $\lambda_{max} \sim 620$ nm and a quantum efficiency $\eta > 90\%$, the optimally doped EL in Alq_3 tends to appear orange, which is due to the contamination of green emission from the host emitter. Although the color saturation can be improved by a higher level of doping, its luminance is greatly compromised due to the onset of concentration quenching. As a result, red color approaching chromaticity coordinates of CIE $x,y=(0.65, 0.35)$ could only be obtained at dopant concentration of higher than 3% when the luminance has dropped well below its plateau. By adding 5% of rubrene as a red emitting assist dopant with 2% DCJTB in Alq_3, Hamada and coworkers at Sanyo [7] was able to achieve a luminance efficiency of 2.1 cd/A with CIE $x,y=(0.64, 0.35)$. Subsequently, the Kodak/Sanyo team discovered [8] that by adding $\sim 6\%$ of NPB as a hole-trapping dopant to the above emitting system simultaneously, the efficiency could further be improved to 2.8 cd/A with a starting luminance of 550 cd/m^2 at 20 mA/cm^2 and near saturated red chromaticity coordinates of CIE $x,y=(0.65, 0.34)$. The encapsulated device structure disclosed

*Corresponding author. Tel.: +886-357-12121; fax: +886-357-50463.
E-mail address: fredchen@eic.nctu.edu.tw (C. H. Chen).

0040-6090/03/$ - see front matter © 2003 Elsevier B.V. All rights reserved.
doi:10.1016/S0040-6090(03)00861-7

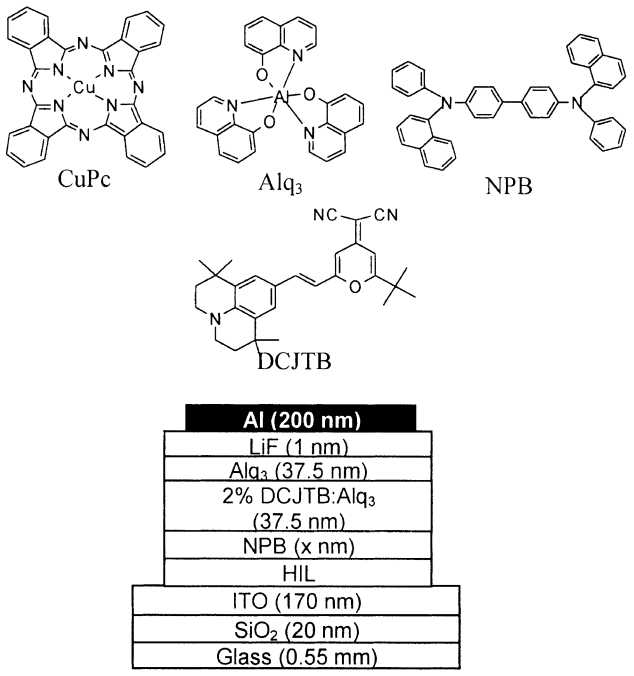

Fig. 1. Structure of doped device and materials.

in that report was [glass/ITO (anode)/150 nm NPB (hole transport)/37.5 nm Alq_3 with dopants (emitter)/37.5 nm Alq_3 (electron transport)/LiF (electron-injecting)/200 nm Al (cathode)] which showed a remarkable projected operational half-life of 8000 h at ambient conditions. It is believed that this EL performance was one of the best for a red fluorescent dye-base OLED emitter including the 1,1′-dicyano-substituted bis(styrylnaphthalene) derivatives (BSN) recently reported by Sony [9].

For full color display, the red emitter of OLED still needs to be improved further to save power consumption and the Kodak/Sanyo's three-dopant process involving DCJTB, rubrene, and α-napthylphenylbiphenyl diamine (NPB) is also in need of simplification. We have restudied the red emitter based on DCJTB and rubrene by varying the hole-injecting materials, film thickness of the hole-transport layer and doping concentration. It was found that the luminance efficiency and color of DCJTB doped emitters can indeed be greatly improved by device optimization without the additional doping of hole-trapping material in the emitter.

2. Experimental

The device architecture was (ITO (170 nm)/HIM (15 nm)/NPB (x nm)/x% DCJTB: Alq_3 (37.5 nm)/Alq_3 (37.5 nm)/LiF (1 nm)/Al (200 nm)) and the structures of materials are shown in Fig. 1, where CuPc and CHF_3 were used as the hole injection materials (HIM), NPB the hole transport material, DCJTB was the red dopant, Alq_3 was the host emitter as well as the electron transport backing layer. The indium-tin oxide (ITO)/glass used was 0.7 mm thick, which contained a passivation layer of 20 nm of SiO_2 and its sheet resistance was approximately 10 ohms/square. In this work, we used two different hole injection materials of 15 nm of copper phthalocyanine (CuPc) and CHF_3 plasma polymerized anode modification layer [10] to study the effect on luminance efficiency.

Prior to organic deposition, the ITO coated glass plate was thoroughly cleaned by scrubbing, sonication, vapor degreasing and oxygen plasma treatment. Devices were fabricated under the vacuum of approximatley 10^{-6} Torr in a thin-film evaporation coater, following a published protocol [11]. All organic layers were prepared by vapor deposition using resistively heated tantalum boats. Typically, the deposition rate was 4 Å/s and the substrate to evaporant source distance was approximately 30 cm. The dopant was coevaporated from resistively heated graphite boat, which was controlled by a temperature controller and monitored through a thermocouple, attached to the side of the boat. By careful control of the dopant boat temperature, it was possible to precisely coevaporate a determined amount of dopant, dispersed into the Alq_3 emitter layer as measured in v/v%. After the deposition of the organic layers and without a vacuum break, the LiF and Al cathode electrodes were deposited in sequence on top of the organic layers using separately controlled sources. The active area of the EL device, defined by the overlap of the ITO and the cathode electrodes, was 0.1 cm^2. The EL emission spectra (taken normal to device) and current–voltage–luminance characteristics of the devices were measured in a dry box with a diode array rapid scan system using a Photo Research PR650 spectrophotometer and a computer-controlled programmable DC source.

3. Results and discussion

To determine if there was any microcavity effect on the coupling out efficiency of the red emission of DCJTB doped device, we began by first studying the basic device architecture using CuPc (15 nm) as the HIM by varying the thickness of hole transport layer (NPB). Fig. 2 shows the plots of EL spectra of 2% DCJTB doped device at various NPB layer thickness that was varied from 60 to 210 nm at 30 nm intervals. The red emission due to DCJTB was found to shift gradually from 624 to approximately 648 nm and back to 630 nm, again as the NPB thickness increases from 60 to 210 nm, with corresponding change of FWHM from 80 to 100 nm to 88 nm. The EL intensities in terms of radiance ($W/Sr/m^2$) were observed also to have changed in a cyclical fashion along with the thickness. This periodicity of emissive pattern can be rationalized by the optical (multiple-beam) interference

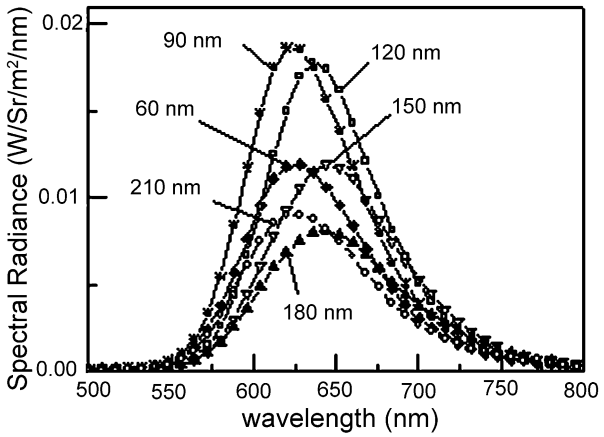

Fig. 2. Effects of NPB film thickness on the EL spectra.

effect [12] caused by the Lambertian nature of the emission, generated in the center of a half-cavity created by the reflective cathode mirror and the transparent ITO/glass substrate in OLED. At lower doping concentration of 0.5% DCJTB, this effect is more prominent as shown in Fig. 3 in which the EL spectrum of the device with thicker NPB of 110 nm shows no residual Alq_3 emission (near 510 nm) while that of the device with 60 nm of NPB is still contaminated with the host green emission due to incomplete Förster energy transfer. From these experiments, the best thickness of NPB layer was therefore determined to be between 90 and 120 nm in consideration of both coupling out efficiency and emissive color.

Although the thicker NPB device of 110 nm can improve the red emission at a lower doping concentration of DCJTB, it was not without cost with CuPc (15 nm) as HIM. As shown in the inset of Fig. 4, the increase of NPB thickness will cause the drive voltage of these devices to rise sharply. By replacing CuPc with

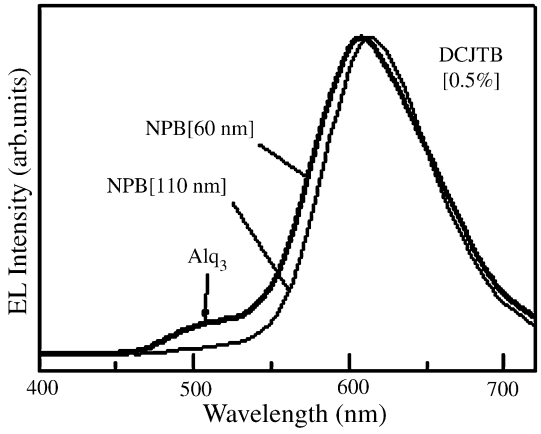

Fig. 3. Comparison of EL spectra of NPB (60 nm) and (110 nm) doped cells.

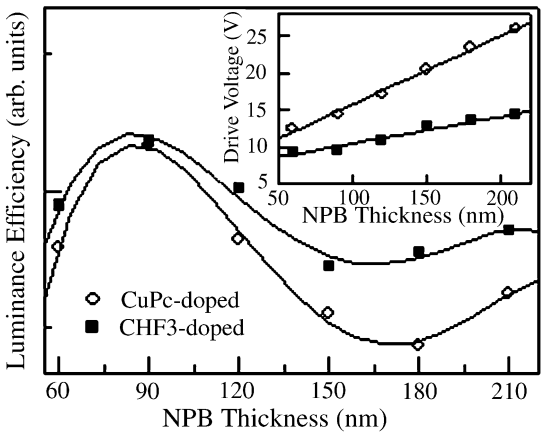

Fig. 4. Current efficiency vs. thickness of NPB layer for CuPc (○) and CHF_3 (■) devices. Inset: drive voltage as a function of the NPB film thickness.

plasma polymerized CHF_3 polymer as hole injection and anode modification layer, the situation can be dramatically improved. By plotting the luminance efficiency against NPB thickness of these two devices, it was noted that the amplitude of periodical variance as revealed in their respective EL efficiency appears also less for the device made of CHF_3 than that of CuPc.

Next we turn to the task of device optimization in attempts to maximize the luminance efficiency (cd/A), power efficiency (lm/W) as well as color saturation of DCJTB doped device in terms of $CIE_{x,y}$ coordinates. This was accomplished by introducing 5% rubrene as the co-dopant along with the systematic change of dopant concentration of DCJTB. The structural variations in device are depicted in Table 1 with common features of anode of (ITO (170 nm)/SiO_2 (20 nm)/glass (0.7 mm)) and cathode of (LiF (1 nm)/Al (200 nm)), omitted for clarification. Fig. 5 shows the plots of luminance yield against doping concentration of DCJTB of all five devices. With NPB at 60 nm and CuPc (15 nm) as HIM, both devices A and B as a group either without or with 5% rubrene co-doping

Table 1
Structural variations in device: glass (0.7 mm)/SiO_2 (20 nm)/ITO (170 nm)/HIL/HTL/EML/ETL/LiF (0.1 nm)/Al (200 nm)

Device	HIL/HTL/EML/ETL
A	CuPc (15 nm)/NPB (60 nm)/Alq_3+DCJTB (*x*%) (37.5 nm)/Alq_3 (37.5 nm)
B	CuPc (15 nm)/NPB (60 nm)/Alq_3+rubrene (5%) +DCJTB (x%) (37.5 nm)/Alq_3 (37.5 nm)
C	CHF_3/NPB(110 nm)/Alq_3+DCJTB (*x*%) (37.5 nm)/Alq_3 (37.5 nm)
D	CHF_3/NPB (110 nm)/Alq_3+DCJTB (*x*%) (30 nm)/Alq_3 (55 nm)
E	CHF_3/NPB (110 nm)/Alq_3+rubrene (5%)+DCJTB (*x*%) (30 nm)/Alq_3 (55 nm)

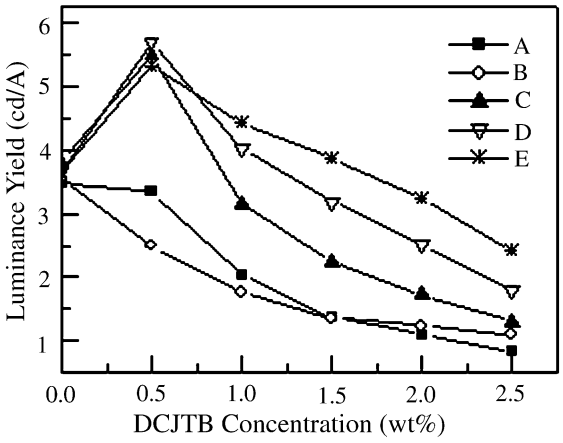

Fig. 5. EL efficiencies as a function of DCJTB doping concentration in Alq_3.

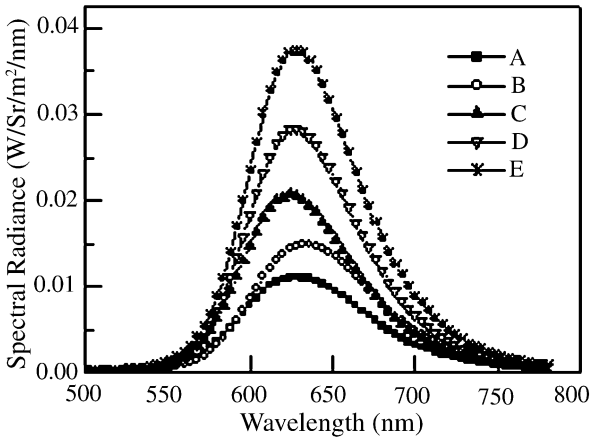

Fig. 6. EL spectra of 2% doped DCJTB devices.

showed dismally low EL efficiency as compared with devices C where NPB was 110 nm, and CHF_3 was used as HIM. Dramatic improvement in luminance efficiency of device C at nearly all doping levels of DCJTB was noted by simply changing the thickness of NPB from 60 to 110 nm without rubrene. Further refinement of the thickness of the doped emitter (to 30 nm) as well as the Alq_3 electron transport layer (to 55 nm) to balance the charge-carriers resulted in further enhancement in efficiency in device D and E. The presence of 5% of rubrene co-dopant in the emitter layer of Device E appeared to prevent the drop of efficiency at higher doping region of DCJTB (from 1 to 2.5%). This is clearly advantageous as a near saturated red emission can be obtained only at DCJTB doping concentration of ~2%. The comparison of overall EL performance of 2% DCJTB doped devices of A–E is thus tabulated in Table 2. The corresponding EL spectra of these devices expressed in spectral radiance of $W/Sr/m^2$ are overlaid in Fig. 6. The best DCJTB doped red OLED device based on the optimized device structure E can achieve a luminance efficiency of 3.24 cd/A at a drive current density of 20 mA/cm^2 with a near saturated color of $CIE_{x,y}$ coordinates of 0.643, 0.354.

Table 2
Overall EL performance of 2% DCJTB doped devices @ 20 mA/cm^2

Device	Lum yield (cd/A)	CIE *x*	CIE *y*	Voltage (V)	Efficiency (lm/W)
A	1.09	0.632	0.363	11.34	0.3
B	1.23	0.648	0.350	11.00	0.35
C	1.99	0.635	0.362	10.28	0.61
D	2.52	0.641	0.356	9.23	0.86
E	3.24	0.643	0.354	8.53	1.19

4. Conclusions

We have successfully fabricated one of the best red DCJTB doped OLED devices where a luminance efficiency of 3.24 cd/A with $CIE_{x,y}$ coordinates of 0.643, 0.354 and a power efficiency of 1.19 lm/W at drive current density of 20 mA/cm^2 and voltage of 8.53 V was achieved. This jump in performance was accomplished by co-doping with 5% rubrene without needing the extra hole-trapping NPB present in the Alq_3 emitter. The dramatic improvement in efficiency is believed to arise from the synergistic effects of increasing the NPB film thickness; replacing CuPc with CHF_3 plasma polymerized hole injection layer as well as balancing of charge-carriers by device optimization. The enhancement of luminous efficiency in red emitter of OLED should prove to be valuable in realization of the full potential of full color OLED as one of the major flat panel displays of tomorrow.

Acknowledgments

We should like to thank the National Sciences Council of Taiwan, R.O.C. for financial support of this research. The generous supply of OLED materials provided by e-Ray Optoelectronics Technology Co., Ltd. is gratefully acknowledged.

References

[1] C.W. Tang, S.A. Van Slyke, C.H. Chen, Appl. Phys. Lett. 65 (1989) 3610.
[2] C.H. Chen, C.W. Tang, Appl. Phys. Lett. 79 (2001) 3711.
[3] J. Shi, C.W. Tang, Appl. Phys. Lett. 80 (2002) 3201.
[4] S. Miyaguchi, S. Ishizuka, T. Wakimoto, J. Funaki, Y. Fukuda, H. Kubota, K. Yoshida, T. Watanabe, H. Ochi, T. Sakamoto, M. Tsuchida, I. Ohshita, T. Tohma, J. Soc. Inf. Display 7/3 (1999) 221.

[5] G. Rajeswaran, M. Itoh, M. Boroson, S. Barry, T.K. Hatwar, K.B. Kahen, K. Yoneda, R. Yokoyama, T. Yamada, N. Komiya, H. Kanno, H. Takahashi, Soc. Inf. Display Dig. 40 (2000) 1.
[6] C.H. Chen, C.W. Tang, J. Shi, K.P. Klubek, Macromol. Symp. 125 (1997) 49.
[7] Y. Hamada, H. Kanno, T. Tsujioka, H. Takahashi, T. Usuki, Appl. Phys. Lett. 75 (1999) 1682.
[8] T.K. Hatwar, G. Rajeswaran, J. Shi, Y. Hamada, H. Kanno, H. Takahashi Proceeding of the 10th International Workshop on Inorganic and Organic Electroluminescence (EL'00), Hamamatsu, Japan, 2000, p. 31.
[9] M. Ichimura, T. Ishibashi, N. Ueda, S. Tamura, Proceeding of the 3rd International Conference EL Molecular Material Relative Phenomena (ICEL-3), O-29, Los Angelos, CA, USA, 2001.
[10] L.S. Hung, L.R. Zheng, M.G. Mason, Appl. Phys. Lett. 78 (2001) 673.
[11] S.A. VanSlyke, C.H. Chen, C.W. Tang, Appl. Phys. Lett. 69 (1996) 2160.
[12] V. Bulovic, V.B. Khalfin, G. Gu, P.E. Burrows, D.Z. Garbuzov, S.R. Forrest, Phys. Rev. B 58 (1998) 3730.